5.4 ATOMIC PHYSICS RESEARCH

T. Nandi

Reshuffling of the beam lines took place last year with the AMS beam line installed in place of atomic physics beamline in LIBR and atomic physics beamline shifted to beam hall II. Although this beam hall is not yet fully ready, we have reinstalled the atomic physics scattering chamber in the line. Detail of this can be found in section 4.5.1. Beam-single-foil and beam-two-foil experiments and inner shell ionization by impact of fast ion beam may start in collaboration with universities again, as soon as beam hall II becomes operational.

Besides the resuming activity in the atomic physics line a Doppler Tuned Spectrometer is being developed indigenously and will be installed in the GPSC. Details are given in section 4.5.2.

Last year before dismantling the beam line all the experiments in the back log were carried out. Most striking result obtained was the observation of prominent non statistical Rydberg states formed during fast ion-atom collisions. In addition to this other salient results are also briefly described below.

5.4.1 Formation of non-statistical Rydberg state from 164 MeV bare Fe-ions colliding with the carbon foil

Nissar Ahmad[1,2], Ranjeet K Karn[2] and T. Nandi[2]

[1] Department of Physics, Aligarh Muslim University, Aligarh-202002
[2] Nuclear Science Centre, New Delhi

Projectile ions traversing through thin foil target may emerge in a variety of excited states. Betz et al [1] proposed that stripped electrons from projectile can be captured even at high Rydberg states of the ionized projectile ions emerging from the foil. We have made an effort to investigate the formation of highly excited Rydberg states in the fast heavy ion-atom collisions. The beam of 164 MeV $^{56}Fe^{12+}$ ions from the Pelletron accelerator was passed through a carbon foil (90 $\mu g/cm^2$) to produce highly charged ions in the excited states. Carbon foil was placed at perpendicular to the beam axis and a germanium ultra low energy (GUL) detector; Canberra having resolution of 150 eV at 5.9 KeV was placed normal to the beam axis. The detector window was equipped with a system of 3 slits at 2.5 mm from the target so that only the delayed x-ray spectrum emanating from excited metastable state of ions produced due to beam foil interaction can be recorded. Normalized beam-foil X-ray spectra obtained at different delay times were plotted to generate the intensity decay curve [2].

A small region of the observed x-ray spectra at different delay time is shown in fig 1. An interesting feature of this spectra is that a line at 6.65 KeV corresponding to three unresolved lines, viz., 1s2p $^3P^0_2$ – $1s^2$ $^1S_0$ (M2) at 6.682 KeV and 1s2s $^3S_1$ – $1s^2$ $^1S_0$ (M1) at 6.636 KeV line in He-like Fe and 1s2s2p $^4P_{5/2}{}^0$ -$1s^2$2s $^2S_{1/2}$ line at 6.619 KeV in Li-like Fe, are seen at smaller delay time. In contrast another line at higher energy side starts showing up at longer delay time and then reaches to a certain maximum before it disappears slowly with time. Normalized intensities of 6.65 and 6.95 KeV peaks have been plotted as a function of distance between the foil and the detector in fig 2. The decay of 6.65 KeV peak (fig.2(a)) follows an exponential nature as expected. However, intensity decay of 6.95 KeV peak shows a peculiar feature as shown in Fig.2(b). At the shorter time scale decay is affected by growing-in effect from short lived cascading levels. The effective lifetime of the growing in levels responsible is found to be about 800 ps. Afterwards decay follows an exponential structure representing a mean lifetime of 1300 ps. A peculiar growth and then decay take place when the exponential decay, representing the statistical decay of a certain level produced at the foil, comes close to the back ground label.

It is very clear from the fig 2(b) that 6.95 KeV line originates due to a short lived as well as a long lived excited state. Long lived state is responsible for the statistical decay. The short lived transition (τ<<1ps) produced at the foil may not reach the detector window. However if the upper state of the short lived transition gets populated right at the detector window then it must sense the radiative transition subsequently. This may be possible by the contribution from long lived cascade levels. Taking this into consideration and the transition energy value suggest us to assign the new line at 6.95 KeV to Ly-α lines involving not only 2s $^2S_{1/2}$ -1s $^2S_{1/2}$ (M1) but also 2p $^2P_{1/2,3/2}$ - 1s $^2S_{1/2}$ (E1). Radiative electron Capture (REC) processes give rise to a structure at high energy side. However it emerges starting from the carbon foil, hence the observed peak at 6.95 KeV appearing at a later time by no means can be attributed to a REC peak.

Theoretical 2p $^2P_{1/2, 3/2}$ level lifetime of 3.498×10^{-15} sec [3] defines decay length ($v \times \tau$) smaller than a μm for velocity of 2.4×10^{10} mm/sec. The level 2 p $^2P_{1/2, 3/2}$ will decay within a few μm. In order to observe the 6.95 KeV line, population of the $1s^2S_{1/2}$ (E1) level must occur right at the detector window. Such a physical situation is only possible if 2p $^2P_{1/2 ,3/2}$ levels get populated on depopulation of high lying Rydberg levels which are produced from the beam-foil interactions and continue to populating the immediate lower levels in succession until they end up to the ground state. Such sequential cascading will lead to various transitions in different wavelength regions. Detection system used in the present experiment works in x-rays domain which can thus monitor the lowest transitions (2p $^2P_{1/2 ,3/2}$ and 2s $^2S_{1/2}$ to 1s $^2S_{1/2}$) in H-like Fe ions.

The Lorentzian structure gives a measure of the time taken for the electrons cascading down from a Rydberg state to 2p $^2P_{1/2, 3/2}$ or 2s $^2S_{1/2}$ state. The time span is about 3700 to 11,800 ps as can be seen in the Fig-2(c). The mean lifetime for an electron in a state characterized by quantum numbers *n* and *l* in the field of a nucleus of charge Z [4], within the non relativistic dipole approximation, is given by

$$\tau\ (n,\ l) = \tau_0\ n^3\ l(l+1)\ /\ Z^4$$

Where τ_0 = 93.42 ps. Assuming the electronic transitions with Δn=1, we have summed up τ_n to obtain the cascading time from n = N to n = 2, with the condition that $\Delta n = \Delta l = 1$. This is done according to Bethe and Salpeter [5] that the oscillator strengths and hence the A co-efficients are numerically much smaller when Δn and Δl are in opposite sense than when they are in same sense. The levels with $l = n$-1 and $l = n$-2 only can satisfy the above criterion, $l = n$-1 levels may land up finally to 2p $^2P_{1/2,\ 3/2}$ state and l = n-2 to 2s $^2S_{1/2}$ states. Lifetimes calculated from above equation show that τ (n=22, l=20, 21), τ (n=23, l=21, 22), τ (n=24, l=22, 23), τ (n=25, l=23, 24), and τ (n=26, l=24, 25) can cause the unexpected peak in the tail of the decay curve of the 6.95 KeV line. Hence, Rydberg levels n = 22 – 26, and l = 20 to 25 are produced in present experimental condition. Such excited states may be produced asymptotically during and after the passage of the projectile through the exit surface of the target foil. Electron capture by multiply charged ions preferentially populates excited states having n=q$^{3/4}$ for projectile charged

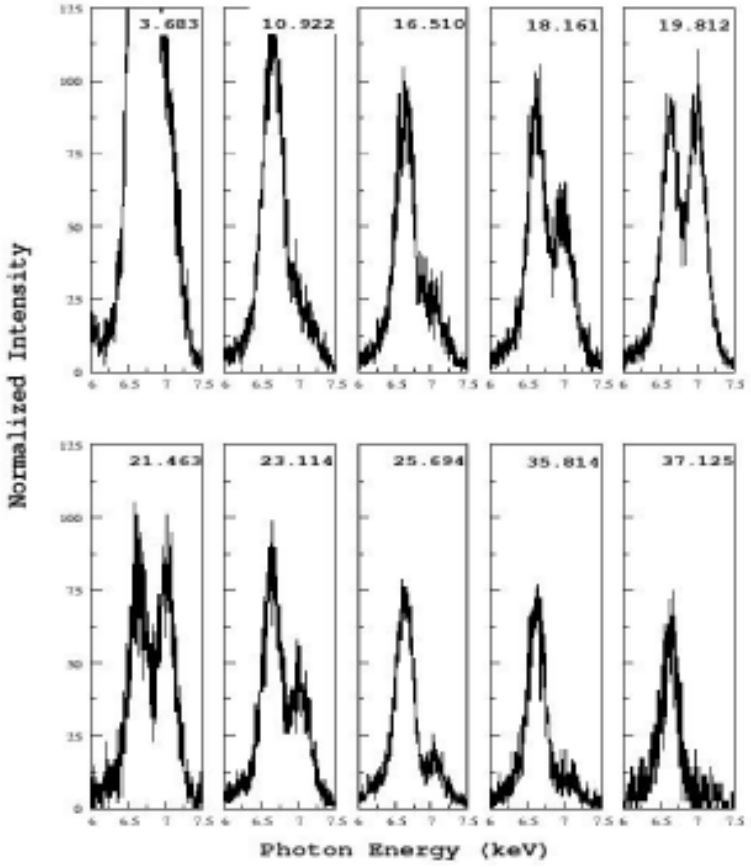

Fig. 1 : A part of the x-ray spectrum of 164 MeV Fe on 90μg/cm^2 carbon foil is shown at different inter detector-foil distance. Spectra show that the peak at 6.95 KeV energy starts appearing around 13 mm and reaches to certain maximum at 24 mm and disappears at about 45 mm. Such variation in normalized intensity of this peak is shown in next figure.

state q [5] where as we have observed $n >> q^{3/4}$. Actual mechanism is not yet known and needs thorough investigations.

Measured exponential decay time is about 3.5 times longer than the 2s $^2S_{1/2}$ level lifetime 350.6 ps [6], which implies heavy cascading effect on it by levels n > 18. At the same instance growing in level lifetime is also a measure of many shorter levels n = 18. Interestingly both cascading and growing effects fed by the statistically produced excited states during the collision. However, the appearance of the peculiar hump may be result from a non statistical process involving levels n = 26-22. Majority is around the level n = 25.

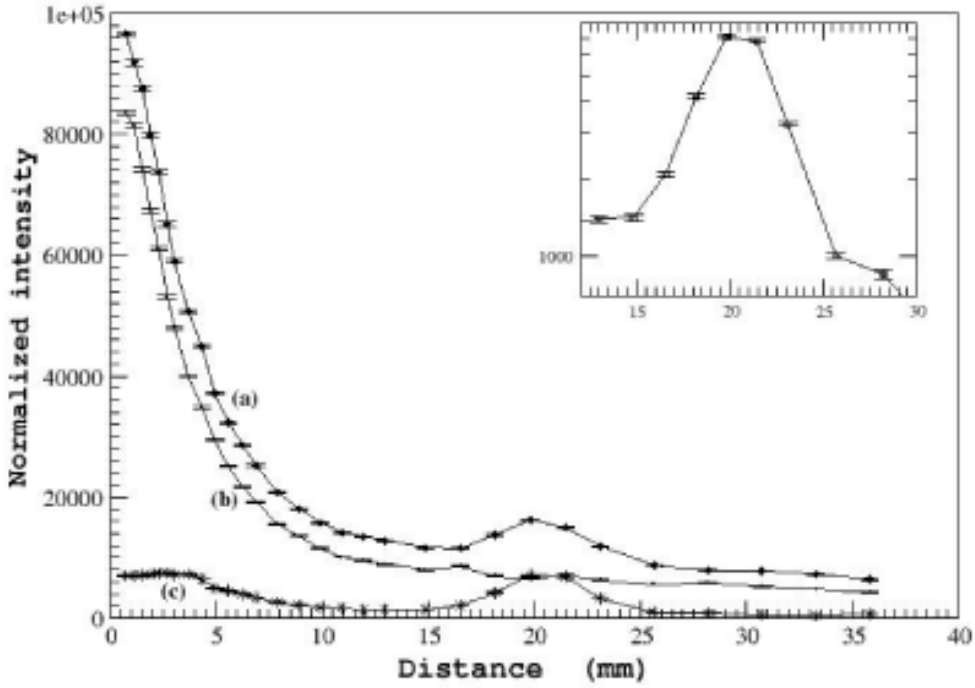

Fig. 2 : X-ray photo peak intensity plot as a function of inter foil-detector distance (a) combined intensity of the two peaks at 6.65 and 6.95 KeV energy, (b) 6.65 KeV peak intensity alone and (c) 6.95 KeV peak intensity alone. The hump appeared in plot (c) is enlarged in the inset.

References:

[1] H.D. Betz, D. Roeschenthaler, and J. Rothermel, Phys.Rev.Lett. 50, 34 (1983).
[2] Nissar Ahmad et al., submitted to NIMB. 2004.
[3] V.G. Pal'chikov and V. P. Shevelko, Reference Data on Multi Charged Ions, Springer Verlag Berlin Heidelberg, 1995.
[4] Hermann Marxer and Larry Spvuch, Phys. Rev. A43, 1268 (1991)
[5] H.A. Bethe and E.E. Salpeter, Quantum Mech. of one- and two -electron atoms.
[6] R.E. Olson, Phys. Rev. A. 24, 1726 (1981).
[7] F.A. Parpia et al. Phys. Rev. A26 (1982) 1142.

5.4.2 Lifetime measurement using a new variant of beam-foil technique

T. Nandi[2], Nissar Ahmad[1] and A. A. Wani[1]

[1] Department of Physics, Aligarh Muslim University, Aligarh-202002
[2] Nuclear Science Centre, New Delhi

The option of varying thickness of the fixed foil in the beam-two-foil technique have been incorporated in our experimental setup utilizing single as well as two-foil target [1]. This gives an opportunity to explore a new mode of the technique. In the current study, the $^{48}Ti_{22}$ ion beam used in the experiment was obtained from the 15 MV Pelletron accelerator at the Nuclear Science Center, New Delhi. A collimated 3 mm diameter $^{48}Ti_{22}$ beam was excited by passage through a 60 μg/cm^2 carbon target movable along the beam. Excited states so generated were passed through a second, fixed carbon foil whose thickness was varied to 4, 8, 12 and 20 μg/cm^2. The experiment was performed with 90, 130 and 145 MeV $^{48}Ti_{22}$ beams in a setup reported elsewhere [2]. Contribution from Li-like 1s2s2p $^4P^o_{5/2}$ is maximum at 90 MeV energy, hence beam-two foil experiment was carried at this beam energy.

Normalized x-ray intensities were plotted as a function of the separation between the two foils (x) (Fig.1) were fitted with the following equation

$$I(x)=I_1\ e^{-x/v\tau 1}+I_2\ (1-e^{-x/v\tau 2}) \quad \text{..... (1)}$$

Here I(x) is the intensity as a function of x. First term represents the decay of the level associated with 4.78 KeV peak. τ_1 was set to a fixed value as obtained from the fit of the single foil data at 90 MeV. Second term is a measure of contribution coming from Li-like 1s2s2p $^4P^o_{5/2}$ to He-like 1s2p $^3P^o_2$ level due to collision at the second foil. Results obtained using different foil are shown in Table 1, in particular, I_2 / I_1 ratio changes with second foil thickness. Mean lifetime agree well with earlier results, details may be found elsewhere [3].

Table-I: Lifetime of the 1s2s2p $^4P^o_{5/2}$ level in Li-like $^{48}Ti_{22}$ obtained from beam single-foil and beam two-foil experiments at 90MeV (4.78 KeV peak). The thickness of the second (fixed) foil was varied.

Foil thickness (μg/cm^2)	*Lifetime (ps)*	*I_2 / I_1*
4	215 ± 16	0.145
8	195 ± 13	0.596
12	183 ± 15	0.706
20	207 ± 14	0.793
Average	200 ± 12	

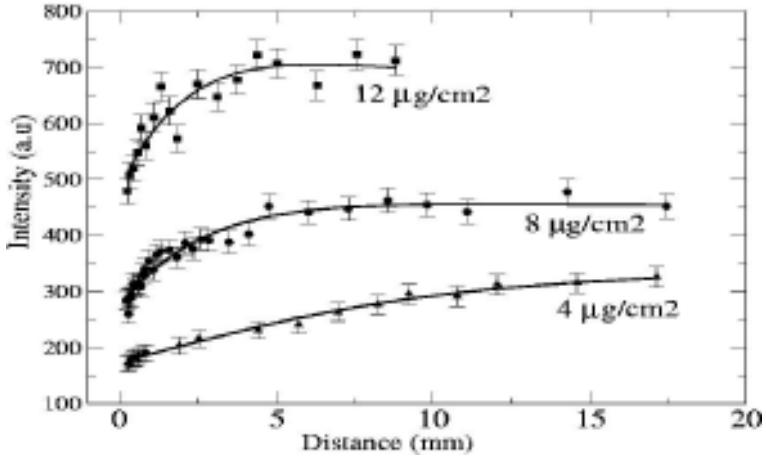

Fig. 1 : Normalized count rate for the 4.78 KeV titanium peak as a function of the distance between the two foils (normalization varies with the foil thickness) in the two-foil experiment. Beam energy 90 MeV, second foil-detector distance 2.5 mm, thickness of the first foil 60 µg/cm^2

REFERENCES

[1] T. Nandi et al., Phys. Rev. A. **66**, 052510 (2002).
[2] Nissar Ahmad et al., submited to Nucl. Instrum. and Methods. (2004).
[3] T. Nandi, Nissar Ahmad, A. A. Wani submited to Phys. Rev. A. (2004).

5.4.3 Effect of satellite lines and hyperfine structure effects on the He-like 1s2p $^3P^o_2$ level lifetime for 17 < Z < 50

T. Nandi

Beam-foil spectroscopy technique is used as an important tool to determine the atomic level lifetime of highly charged ions in many laboratories. This technique suffers from blending problem, for example, in the measurements where the satellite is not resolved and no other means are used to consider contribution of two neighboring charge states, the measured lifetime of the He-like 1s2p $^3P^o_2$ level can be considered as a weighted average ("effective") of the lifetimes of the He-like 1s2p $^3P^o_2$ and the Li-like 1s2s2p $^4P^o_{5/2}$ states. Further when a swift-ion beam passes through a foil, several charge states are generated with different fractions and therefore the "effective" lifetime depends on the actual fractions of He- and Li-like ions present in the beam exiting the foil. In addition, the branching ratios for the decay of the 1s2p $^3P^o_2$ and 1s2s2p $^4P^o_{5/2}$ levels via M2 are of importance, since other decay channels also exist via E1-transition ($1s2p^3P_2{}^0$–1s2p $^3P^o_2$) and electron emission $1s^2\ ^1S_0$ -1s2s2p $^4P^o_{5/2}$, respectively. The "effective" lifetime of the 1s2p $^3P^o_2$ level may therefore be written as

$$\tau_{eff} = ((g1x\ BR1\ x\ \tau_1) + (g2\ x\ BR2\ x\ CFR\ x\ \tau_2)) / (g1\ x\ BR1+(g2\ x\ BR2\ x\ CFR))$$

where g1 and g2 are the statistical weight of the 1s2p $^3P^o_2$ and 1s2s2p $^4P^o_{5/2}$, BR1 is the M2 branching ratio of the 1s2p $^3P^o_2$ state, BR2 is the x-ray M2 branching ratio of the 1s2s2p $^4P^o_{5/2}$ state, and CFR is the charge-state fraction ratio of Li-like to He-like ions in the foil-excited beam. CFR has been obtained from the code ETACHA [1]. In the ETACHA, data for thickness of the carbon foils, incident beam energy, and initial charge states were taken from the original publications. Effective lifetimes estimated from equation (1) are assumed to have an error of 10% mainly arising from CFR results.

Calculations agree reasonably well in all cases with the measured data. Now we will make an attempt to include the effect of hyperfine structure (HFS) in addition to satellite effects. One can see that the He-like V 1s2p $^3P^o_2$ lifetime agrees well with theoretical value if HFS effects are not considered [2]. In contrast one may see that the Li-like V 1s2s2p $^4P^o_{5/2}$ lifetimes are much shorter than the theoretical lifetime without HFS effects. To compare these measured lifetimes of He-like 1s2p $^3P^o_2$ and Li-like 1s2s2p $^4P^o_{5/2}$ V [2] are taken to estimate the effective lifetime from the semi-empirical formula mentioned above. Experimental lifetimes are chosen because no theoretical calculation exists for Li-like 1s2s2p $^4P^o_{5/2}$ level lifetime including HFS. Semi-empirical calculations for effective lifetime of He-like V 1s2p $^3P^o_2$ are compared with measured values, at different beam energies, showing good agreement.

The study shows that HFS can cause the reduction of lifetime where as satellite blending can increase as well as decrease lifetime depending on atomic number. Therefore, these two effects need to be resolved. Details can be found elsewhere [3].

REFERENCES

[1] J.P. Rozet, C. Stephan, and D.Vernhet, Nucl.Instrum. Methods. B107, 67(1996).

[2] T. Nandi, P. Marketos, P. Joshi, R. P. Singh, C. P. Safvan, P. Verma, A. Roy. A. Mandal, and R. K. Bhowmik, Phys. Rev. A66, 052510(2002).

[3] T. Nandi, Euro. Phys. J. D. submitted (2004).

5.4.4 Photon Emissions from Ion Collisions with Microdroplets

G.K. Padmashree, C.P. Safvan, D. Kanjilal and A. Roy

Liquid microdroplets are high-density, bulk-like, micron-size, spatially-confined macroclusters, which form fascinating mesosystems. These novel targets make accessible, the hitherto unavailable target densities to probe and explore the gradual transition of matter from atomic/molecular level to the bulk level. While the large local density in a microdroplet gives rise to bulk-like behavior, the small size and spatial confinement ensure that atomic/molecular effects do not lose their relevance. The coexistence of these two separate aspects corresponding to different density regimes is one of the reasons for the interest in research with microdroplets. Ion collisions with liquid microdroplets is an area of research that has just emerged. The feasibility of these experiments has been successfully

tested out by us, by developing and implementing the know-how for introduction and removal of microdroplets in a high-vacuum environment as targets for collisions with energetic ions.

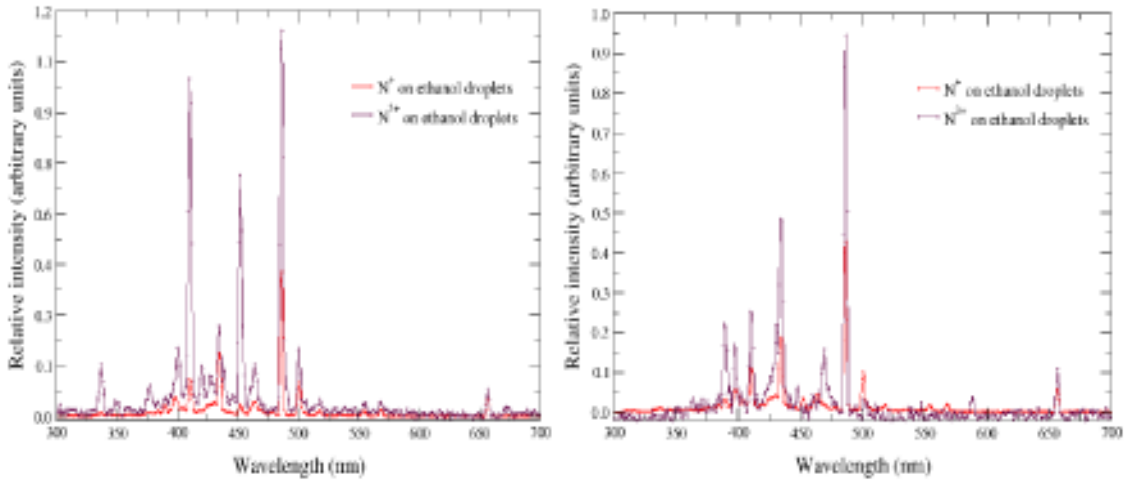

Fig. 1 : Optical spectra from collision of N^{q+} with ethanol droplets

Ethanol microdroplets (of about 15-17 micron diameter) have been generated by uniform break up of ethanol microjet using a piezocrystal-driven microcapillary (PDM) tube. Droplet train, ion beam and the photon detector are mutually perpendicular. Ultraviolet (UV) and visible photon emissions during the interaction of these microdroplets with 150q keV energy N^{q+} ions (q+ is the charge state of the ion) from an electron-cyclotron-resonance (ECR) ion source placed on a high-voltage platform, were monitored. A photomultiplier tube (PMT) sensitive to wavelengths in the range 300 nm to 650 nm with peak sensitivity at 420 nm, coupled to the exit slit of a diffraction grating-based monochromator in Czerny-Turner configuration, together with signal processing and data acquisition systems, comprised the photon detection system. The optical spectra resulting from collision of N^{q+} with ethanol droplets are shown in Figure 1.

The fundamental processes like ionization, excitation and electron capture that are known to occur in ion collisions with conventional targets like atoms, molecules, small clusters and surfaces are accompanied by photon emissions. Intuitively, such processes are expected to occur in ion interaction with microdroplets. All of the above processes are strong sources of photons since the excited states which subsequently decay through photon emissions, are mainly populated. While a direct deexcitation to one of the vacant lower energy levels results in the emission of an x-ray photon, a sequential deexcitation through intermediate energy levels will result in an emission cascade with transition energies lying mostly in the ultraviolet (UV) and visible region of the electromagnetic spectrum. In the experiments with microdroplets, this feature stems from the multitude of relaxation pathways available for the excited ion-droplet complex. The catalog of UV and visible emission lines in the photon spectra serve as tell-tale fingerprints of the collisional interaction, and aid in the diagnostics of the fundamental mechanisms.

Distinct processes like ionization, excitation, single electron capture, double, triple and multiple electron capture have been identified with UV/visible photon emissions from the collisional interaction mentioned above. The spectral lines from the interaction of highly charged nitrogen ions (N^{5+} and N^{6+}) are prominent in collisions with droplets indicating that these high-density bulk-like targets offer a sea of the electrons. The optical emissions from transitions involving inner shell or core excitations of the projectile have fairly large intensities in ion-droplet collisions. These transitions are otherwise less probable, for instance, in low-density targets like molecules. Multiple collisions within the droplets have lead to the increased probability of such excitations.

The nature of inelastic processes like ionization, excitation, single and double electron capture that have been identified with these photon emissions are suggestive of a molecule-like behavior of the massive droplet. The reneutralization of highly charged projectiles due to the multiple electron capture processes that are highly probable with these high-density targets, as opposed to molecular targets, point to a bulk-like behavior of the microdroplets.